Carrier dynamics in quantum dot lasers

A. Fiore[1], A. Markus and M. Rossetti
Ecole Polytechnique Fédérale de Lausanne (EPFL)
Institute of Photonics and Quantum Electronics - CH-1015 Lausanne (Switzerland)

ABSTRACT

We analyze the impact of slow intraband relaxation and strong carrier localization on the characteristics of quantum dot (QD) lasers. Relatively long intraband relaxation times and population filling of the QD ground state lead to carrier pile-up on excited states, reducing the laser efficiency and maximum output power. Strong carrier localization in the QDs and consequently large thermal hopping time within the QD ensemble results in the absence of quasi-thermal equilibrium under lasing conditions, as evidenced by stimulated and spontaneous emission spectra. The impact of these specific physical characteristics of QD active regions on the laser high-frequency modulation properties is analyzed, particularly with regards to the differential gain, the gain compression and the linewidth enhancement factors.

Keywords: Quantum dot lasers, differential gain, gain compression factor, linewidth-enhancement factor.

I. INTRODUCTION

After over ten years of material development, quantum dot (QD) lasers are now a strong competitor to the commercial quantum well (QW) based technology for several applications. QD edge-emitting lasers at 1300 nm on GaAs substrates exceed the performance of InP-based QW edge-emitters in many important parameters, such as threshold current, temperature stability, chirp and feedback insensitivity. They may thus find application in low-cost 10 Gb/s transmitter modules, by releasing the need for temperature controllers, isolators and external modulators. However, the frequency response of 1.3 μm QD lasers appears to be limited (to values in the order of 7-8 GHz) by the small differential gain ($\approx 10^{15}$ cm^{-2}) and the large K factor (1-4 ns) [1-4], which have been attributed to slow carrier capture and spectral hole burning [5, 4]. In contrast, much higher modulation frequencies up to 15 GHz have been obtained in QD lasers operating at ≈1 μm by using tunnel injection [6]. It is thus clear that intraband relaxation processes, including capture and intradot relaxation, and nonequilibrium carrier distribution (and thus spectral hole burning) in the QD ensemble play a major role in the laser dynamics, with important consequences on possible applications. In this paper, we examine this problem from a broader point of view, by modeling several experimental observations related to intraband relaxation and nonequilibrium effects. The comparison between modeling and experiment provides a detailed understanding of these processes and allows us to estimate some of the key material parameters (relaxation and capture times). This in turn leads to a simple understanding of the main limiting factors in the amplitude and phase response of a QD laser under small-signal modulation, including an analytical expression of the differential gain and gain compression factor, and provides routes for the optimization of the frequency response. In particular, we will show that the main limiting factor in the dynamics is the intraband relaxation between excited state (ES) and ground state (GS).
The paper is structured as follows: In the introduction a general description of the processes affecting the dynamic response is given. Section II focuses on carrier capture and intraband relaxation. Section III discusses quasi-equilibrium and spectral-hole burning in the QD ensemble. In section IV the impact of capture and relaxation on the dynamic response is discussed. Laser parameters (areal densities, relaxation times, …) corresponding to strongly-confined InAs/GaAs QDs emitting around 1300 nm will be considered throughout.

[1] Email: andrea.fiore@epfl.ch. Permanent address: Institute of Photonics and Nanotechnology, CNR, Via del Cineto Romano 42, 00156 Roma (Italy)

Photonic Materials, Devices, and Applications, edited by
Gonçal Badenes, Derek Abbott, Ali Serpengüzel, Proc. of SPIE Vol. 5840
(SPIE, Bellingham, WA, 2005) · 0277-786X/05/$15 · doi: 10.1117/12.608478

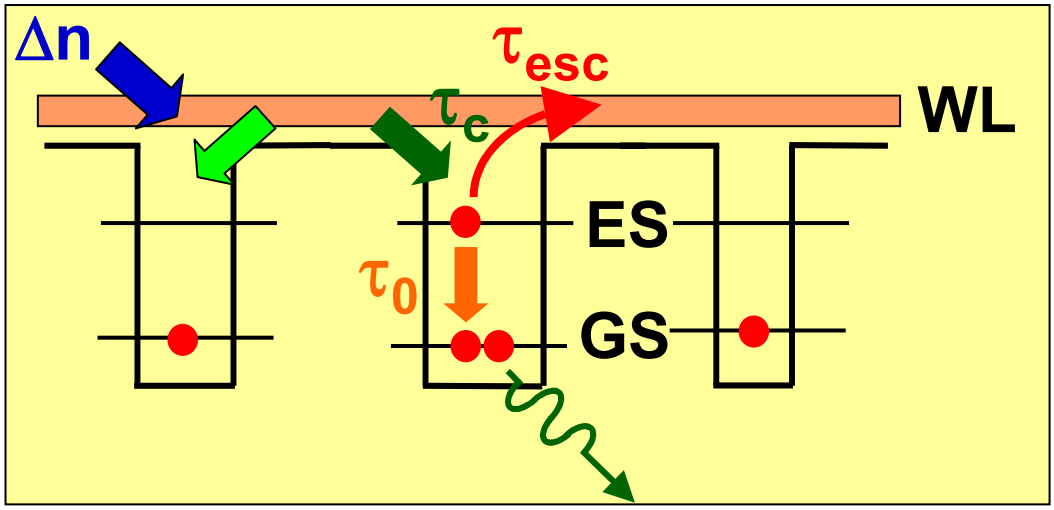

Fig. 1: Schematics of carrier pile-up in QD lasers

Our starting point is that QD lasers are subject to carrier pile-up in nonlasing states due to the limited density of states, the relatively slow (≈few ps) intradot relaxation, and the large thermal hopping time (see Fig. 1). When additional carriers are injected into the active region, e.g. during laser modulation, they relax to the GS by capture from the two-dimensional wetting-layer (WL) into the ES of the dot, then relaxation from the ES to the GS. The GS can accommodate a maximum of two electron-hole (eh) pairs, with a corresponding maximum modal gain of ≈3-4 cm^{-1} per QD layer for state-of-the-art areal densities of 3-4x10^{10} cm^{-2}. This implies that for typical cavity losses QD lasers operate relatively close to GS population filling. The ES to GS effective relaxation rate is thus reduced by the Pauli-blocking factor $\left(1-f_{GS}\right)$,

$$\left.\frac{df_{GS}}{dt}\right|_{rel} = \frac{f_{ES}\left(1-f_{GS}\right)}{\tau_0}$$

where f_{GS}, f_{ES} are the GS and ES occupation probabilities, and τ_0 the relaxation time for an empty GS. In continuous-wave operation, as the current and thus the stimulated emission rate is increased above threshold, the ES population must increase to sustain the increased supply of carriers to the GS through relaxation. As it will be shown in the following, this incomplete clamping of the QD population leads to reduced internal quantum efficiency, and eventually to a complete saturation of the GS output power when the ES gain reaches threshold and stimulated emission from the ES starts competing with relaxation [7]. Moreover, carrier pile-up in the ES leads to a strongly asymmetric gain profile, and therefore to large linewidth-enhancement factor α [8], making the ideal picture of α=0 totally invalid. In dynamic operation, the limited relaxation rate implies that only a fraction of injected carriers will contribute to additional gain from the GS, whereas some will remain on higher-energy states - this results in a reduction of differential gain, and therefore of the relaxation oscillation frequency, as it will be shown below. Slow intraband relaxation also produces gain compression – i.e. the reduction of gain *at constant total carrier population* for increasing optical intensity – and therefore impacts the damping in the frequency response through the K-factor. We note that slow capture can also reduce the differential gain and increase the gain compression factor through the same mechanisms, as suggested previously [5, 4]. However, capture in the QD is not affected by GS filling due to the large number of available ES in the strongly-confined QDs emitting at 1300 nm. Experimental data showing the carrier pile-up in the ES will be presented in Section II to confirm that ES to GS relaxation, rather than capture, is the main limiting process. A quantitative analysis of the effect of relaxation and capture on differential gain and K factor will be given in Section IV.
One additional damping process arises due to the inhomogeneous nature of the QD ensemble. Indeed, electrons residing in QDs with energies away from the lasing line do not necessarily contribute to the stimulated emission process. The

fraction of lasing QDs is fixed by the ratio $\Gamma_{hom}/\Gamma_{inh}$ of homogeneous to inhomogeneous broadening (if $\Gamma_{hom}/\Gamma_{inh}>1$ essentially all dots interact with the cavity photons), and by the relative rates of carrier transfer among dots and stimulated emission (if the thermal hopping is much faster than the stimulated emission rate, a quasi-equilibrium situation is established in the QD ensemble, which therefore acts as a single population). In Section III we derive some of these parameters from the comparison of spontaneous and stimulated emission spectra and show that quasi-equilibrium is not reached under lasing operation. The corresponding spectral hole burning affects the differential gain and gain compression factor, and should be considered in evaluating the dynamic properties.

II. INTRABAND RELAXATION IN QD LASERS

The effect of limited intraband relaxation rate is apparent when investigating the emission of QD lasers operated well above threshold [7]. If lasing on the GS is obtained with a relatively large GS threshold population (i.e. close to gain saturation), a second lasing line arising from the ES transition is observed when increasing the current well above threshold (see Fig. 2(a)).

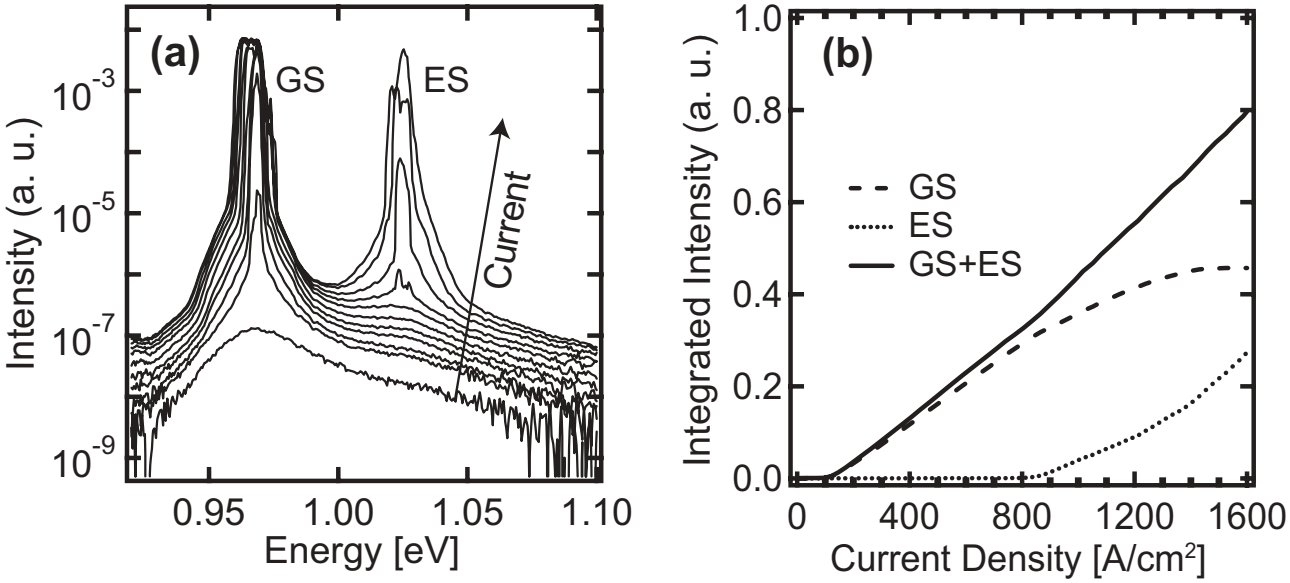

Fig. 2: (a) Lasing spectra at different currents for a 2 mm-long laser with 3 layers of QDs. (b) Integrated intensities of GS and ES lasing lines versus current density.

By spectrally resolving the emission of the two states (Fig. 2(b)), the existence of a clear laser threshold for the ES transition is observed. Above the ES threshold, the GS emission is essentially saturated, which shows a competition between stimulated emission from the ES and relaxation to the GS. This intriguing two-state lasing behavior can be understood on the basis of the intraband relaxation process depicted in Fig. 1: Due to the finite relaxation time τ_0, the increase in relaxation rate - needed to sustain the increasing GS stimulated emission rate – implies an increasing ES population. At some point the ES gain reaches the threshold value and lasing from the ES starts. From this point on, as the ES population must remain clamped to its threshold value, no increase in the relaxation rate is possible, and the GS stimulated emission rate (and thus the output power at the GS energy) cannot increase with current. This intuitive picture is confirmed by the calculation of GS and ES population and cavity photon number (Fig. 3) in a simple rate-equation model where the different processes of capture, relaxation, and thermal re-excitation are taken into account [7, 9] (the carrier injection rate on the x-axis is defined as the number of carriers injected per QD and per lifetime).

The ratio of ES to GS threshold is very sensitive to the value of τ_0 and of the cavity loss, and a single value of $\tau_0 \approx 8$ ps has allowed us to fit this ratio for different cavity losses [7]. On the other hand, the two-threshold behavior is basically independent of the capture time, since the latter determines the extent of carrier pile-up in the wetting layer but does not influence the intradot dynamics. The observation of carrier accumulation on the ES is a direct evidence of the fact that a bottleneck exists in the relaxation between ES and GS, with important consequences on the GS maximum output power, internal quantum efficiency (carrier pile-up on the ES reduces the differential efficiency above threshold), and, as it will

be shown in Section IV, on the frequency response. The detrimental effect of slow intraband relaxation can be avoided by increasing the effective relaxation rate $(1-f_{GS})/\tau_0$, i.e. by reducing the GS threshold occupation factor or the relaxation time. Increasing the number of dots or decreasing the cavity loss indeed results in a lower GS and ES population at threshold, suppresses the two-state lasing mechanism and improves the differential gain. The intraband relaxation time is determined by phonon scattering and by Auger processes, whose rates are complex – and not yet well understood - functions of QD energy spectrum and population.

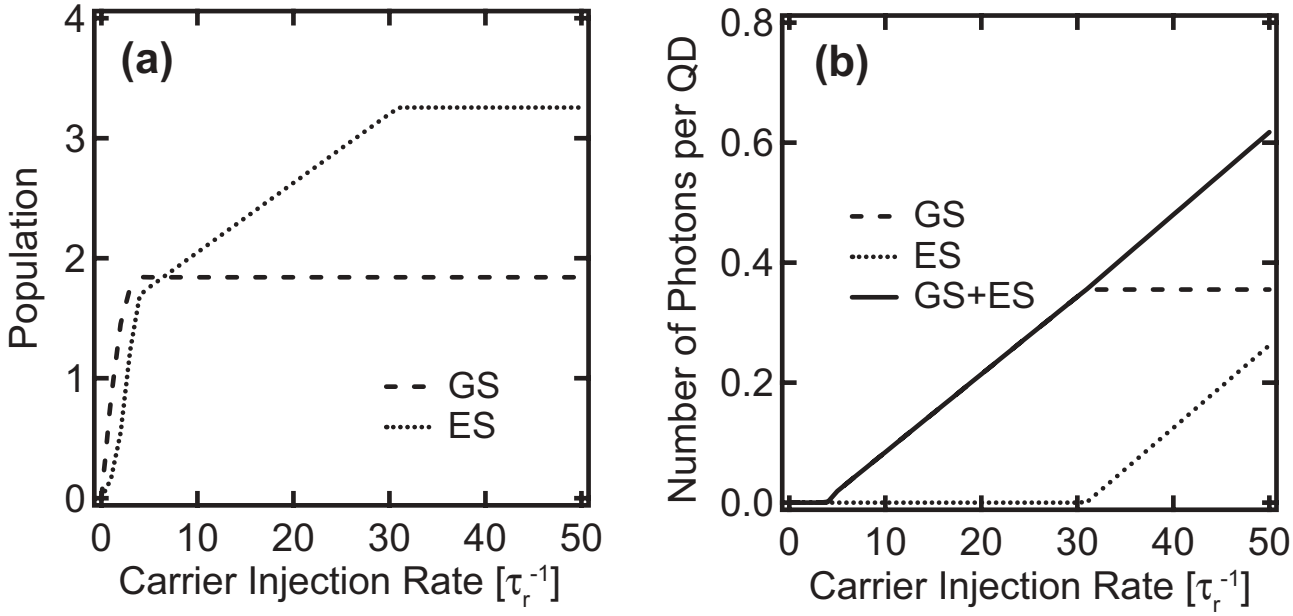

Fig. 3: Population (a) and cavity photon number per QD (b) in a 2 mm-long laser with 3 layers of QDs, calculated with a rate equation model assuming τ_0=8 ps.

III. THERMAL HOPPING AND QUASI-EQUILIBRIUM IN THE QD ENSEMBLE

The carrier distribution in the QD ensemble can be thermal or non-thermal, depending on the relative rates of interdot carrier hopping and interband recombination processes. Hopping (Fig. 1) is limited by thermal escape time τ_{esc} from the ES to the WL, which in turn is related to the capture time τ_c. These times are difficult to measure directly, however an order-of-magnitude estimate can be provided by a careful analysis of the spectral characteristics of QD lasers. To this aim, we have measured the lasing and spontaneous emission (SE, from a window in the top contact) spectra in a 2 mm-long laser with 3 QD layers (see Fig. 4(a)).

By comparing stimultated emission (Fig. 2(a)) with SE spectra (Fig. 4(a)) Two important features are observed: (1) The lasing lines from both GS and ES broaden significantly with increasing current above threshold (as apparent in Fig. 2(a)). This indicates that an increasing number of QDs reaches threshold with increasing current and thus that the QD ensemble is not completely in quasi-thermal equilibrium. In the limit of negligible homogeneous broadening and long thermal escape time the QDs in the ensemble do not form a unique population but rather reach threshold and lase almost independently (this is indeed observed at low temperatures [10]. (2) The lasing peak from the ES is red-shifted as compared to the SE peak. This is on the other hand a hint of a partial carrier transfer taking place among QDs, which favors the population of low-energy QDs and therefore red-shifts the gain peak as compared to the spontaneous emission (due to their different dependence on the occupation factors). In order to quantitatively explain the observed behavior, the lasing process in the QD ensemble can be modeled [11] by slicing the inhomogeneous spectrum of the QD ensemble in energy intervals and writing rate equations for the populations and photon numbers in each interval. The gain and SE spectrum of each interval is then convoluted with a Lorentzian lineshape to include the effect of homogeneous broadening. Carrier hopping among QDs is naturally included as thermal escape to the WL and subsequent re-capture. The main fitting parameters in the model are – besides relaxation times which are fixed to ≈10 ps

from the discussion in Section II – the electron and hole capture times and the homogeneous broadening Γ_{hom}. This "multimode" rate equation model can reproduce [12] the experimental lasing and SE spectra by assuming a capture time $\tau_c \approx 1$ ps.

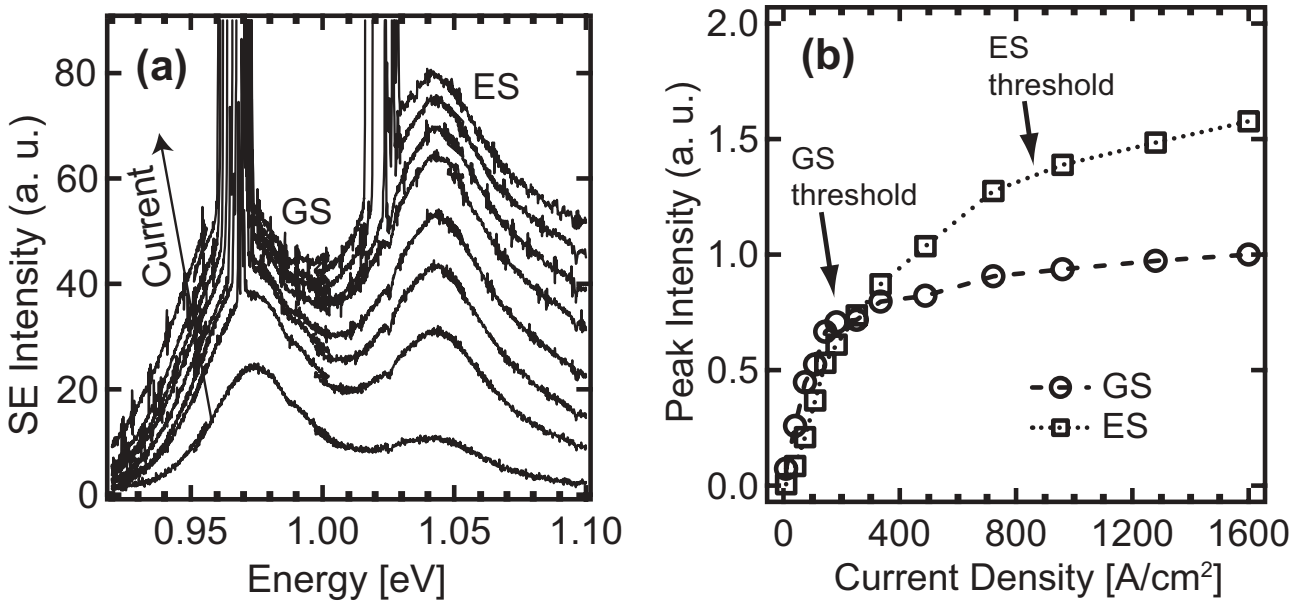

Fig. 4: (a) Electroluminescence from a window in the top contact for different currents at room temperature. (b) Peak intensity (GS and ES) of the SE spectra from the holes in the top contact as a function of current density.

A further indication about the extent of interaction among carriers residing in different QDs can be derived from the analysis of the saturation behavior of the SE above lasing threshold. Figure 4(b) shows the SE peak intensities at GS and ES energies (from the top-emission spectra on the right side of Fig. 4(a)) as a function of current density. In contrast from the simple picture presented in Section II (Fig. 3(a)), where populations are expected to clamp at their respective thresholds, the spontaneous emission from GS and ES keeps increasing above threshold, although at a smaller rate.

The incomplete clamping of GS and ES SE is a consequence of incomplete quasi-thermal equilibrium and homogeneous broadening. As the population of QDs off the gain peak increases above threshold, their contribution to SE at the lasing energy (through the homogeneously broadened lineshape) also increases, leading to increasing SE intensity. This behavior strongly depends on the values of the homogeneous broadening and capture time. Assuming $\Gamma_{hom} \approx 8$ meV and $\tau_c \approx 1$ ps indeed allows us [12] to reproduce the experimental dependence in the multimode rate equation model (Fig. 5(a)).

Using these values of Γ_{hom} and τ_c, we can calculate the electron and hole distribution functions in the QD ensemble below and above threshold (Fig. 5(b)), and discuss the quasi-equilibrium issue more quantitatively. The hole distribution closely follows a Fermi-like distribution, with only shallow holes in correspondence to the lasing energies. In contrast, the electron distribution is strongly non-thermal both below and above threshold, and shows significant hole burning at both GS and ES lasing energies. The difference is of course related to the much larger potential heterobarriers in the conduction band, resulting in longer thermal escape times (identical capture time 1 ps is assumed from electrons and holes).

The quantitative modeling of stimulated and spontaneous emission spectra in QD lasers thus allows us to conclude that quasi-thermal equilibrium is not completely achieved, particularly in the conduction band, due to the strong electronic confinement in the QDs. This should be contrasted to the case of quantum wells, where intraband scattering processes between different k-states are much faster, and produce a carrier distribution closer to thermal equilibrium, at least at low light intensities. It can be thus expected that spectral hole burning will play an important role in the dynamic characteristics of QD lasers, particularly with respect to the gain compression factor, as already pointed out in Ref. [5].

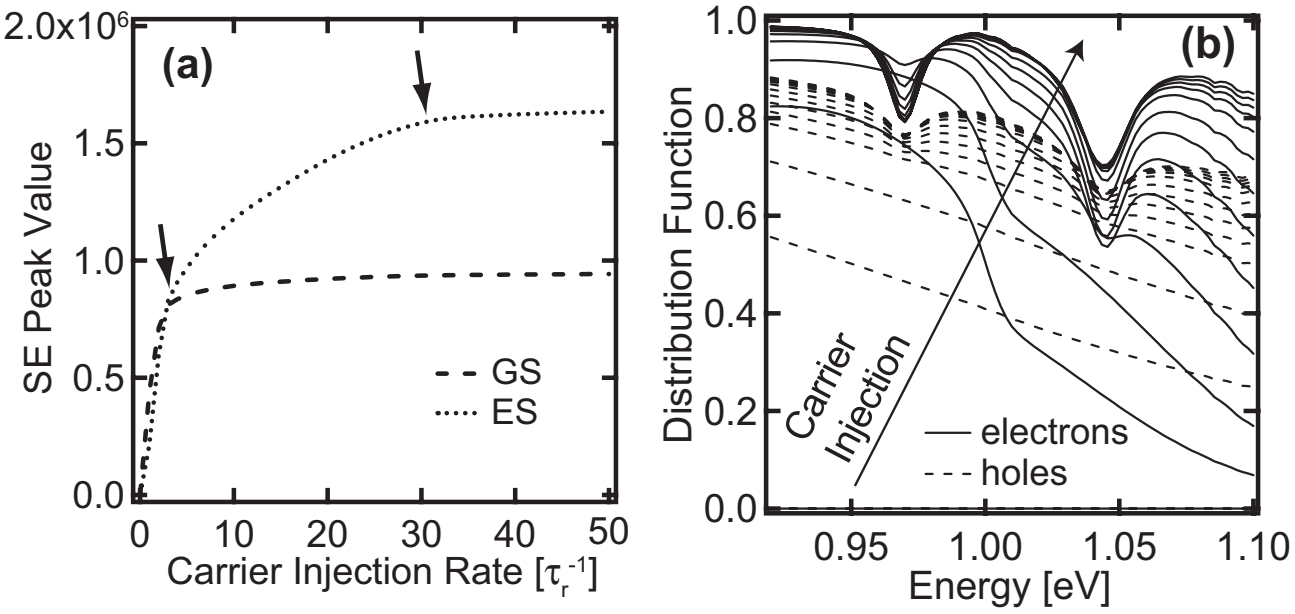

Fig. 5: (a) Calculated values of the SE photon number vs injection rate. The GS and ES threshold values are indicated by arrows. (b) Calculated electron (full lines) and hole (dashed lines) distribution functions for various injection level below and above threshold, assuming $\Gamma_{hom} \approx 8$ meV and $\tau_c \approx 1$ ps

IV. IMPACT OF CAPTURE AND RELAXATION ON THE MODULATION CHARACTERISTICS

The dynamic response of QD lasers can be calculated in the time-domain by numerical solution of the time-dependent rate equations [8], or by linearization, Fourier transform and solution in the frequency domain, in the small-signal approximation. However, it is useful to extract the key device parameters (differential gain, gain compression factor), examine their dependence on the material parameters, and compare them with bulk or quantum well devices. This can be done by solving the intraband dynamics in a quasi-static approximation, i.e. assuming it is much faster than the interband recombination times, to extract the differential gain $a = \left.\frac{\partial g_{GS}}{\partial N_{tot}}\right|_{N_p}$, and the gain compression factor, or (more conveniently) the derivative of gain with respect to the photon density at constant carrier density: $a_p = \left.\frac{\partial g_{GS}}{\partial N_p}\right|_{N_{tot}}$. In these expressions, g_{GS} is the GS modal gain, N_{tot} is the total density of carriers (GS, ES and WL), and N_p is the photon density. The small-signal frequency response is then easily calculated using standard semiconductor laser theory by treating the interaction of the photons with the total carrier density [13],

$$H(f) = \frac{\partial N_p}{\partial I} \propto \frac{1}{f_r^2 - f^2 + j(\gamma/2\pi)f}$$

where $f_r^2 \simeq \frac{v_g a}{4\pi^2 \tau_p} N_p$, $\gamma \simeq \frac{1}{\tau_{\Delta n}} + K f_r^2$, $K = 4\pi^2 \tau_p \left(1 + \frac{\Gamma a_p}{a}\right)$

and v_g is the group velocity, τ_p the photon lifetime, $\tau_{\Delta n}$ the diffential carrier lifetime, and Γ the confinement factor. While this separation of intraband and interband dynamics is an approximation which neglects the role of additional zeros and poles introduced in the frequency response by the intraband processes, it gives results very close to the complete numerical calculation in the parameter range analyzed in the following. By linearizing the rate equations in the

single mode model (the effect of spectral hole burning is not considered here) and imposing a *steady-state* condition within the band, analytical expressions for a and a_p are easily found, which are functions of the laser bias point.
We first focus on the differential gain a. In order to separate the effects of capture and relaxation, we write it as:

$$a = \left.\frac{\partial g_{GS}}{\partial N_{tot}}\right|_{N_p} = g_0 \left.\frac{\partial N_{GS}}{\partial N_{QD}}\right|_{N_p} \left.\frac{\partial N_{QD}}{\partial N_{tot}}\right|_{N_p} = g_0 a_r a_c$$

where g_0 is the gain per eh-pair in the GS (assumed to be constant), N_{GS} is the ground state population, $N_{QD}=N_{GS}+N_{ES}$ is the population in the QD, including GS and ES. The two adimensional parameters a_r and a_c represent the relative variation of the GS and total QD population, and depend on the efficiency of the relaxation and capture processes, respectively. Figure 6 presents the values of a_r, a_c (Fig. 6(a)) and a (Fig. 6(b)) as a function of injection rate in a 500μm long, laser with 10 layers of QDs, with high-reflectivity coatings (R_1=0.8, R_2=0.95), taken from Ref. [14], where 10 Gb/s modulation was demonstrated. The gain per carrier g_0, capture time τ_c=1 ps and relaxation time τ_0=8 ps have been taken from our measurements on lasers with similar QD active regions. The relatively low value of the differential gain and its strong decrease with current above threshold are clearly related to the relaxation bottleneck: most carriers injected in the WL do not relax down to the GS to contribute to gain but rather accumulate in the ES – as discussed in Section II. While this conclusion depends on the values assumed for the capture and relaxation times, and on the GS filling at threshold, we have verified that relaxation remains the limiting factor in the differential gain in the parameter range $\tau_c<10\tau_0$, which covers all experimental values in the literature. The main reason for this is of course the role of Pauli-blocking due to GS filling in reducing the effective relaxation rate from the ES to the GS. We also note that a more accurate model should include higher-energy states, which would reduce even further the role of carrier capture (Pauli blocking does not affect the capture process because there are always available states in the QD). This conclusion on the dominant role of intradot relaxation in limiting the differential gain contrasts with previous theoretical results [5, 4], which have neglected the presence of ES, and indicates that attempts to improve the laser dynamics should focus on reducing the relaxation time τ_0 (by engineering the ES energy position and wavefunction) or to direct tunnel injection *into the GS*. Finally, it is clear that the decrease of the differential gain with injection above threshold is an evidence of gain compression, i.e. of an evolving carrier distribution in the QD at increasing optical intensities: As discussed in Section II, increasing stimulated emission rate from the GS implies an increasing ES population and a further reduction in the differential gain.

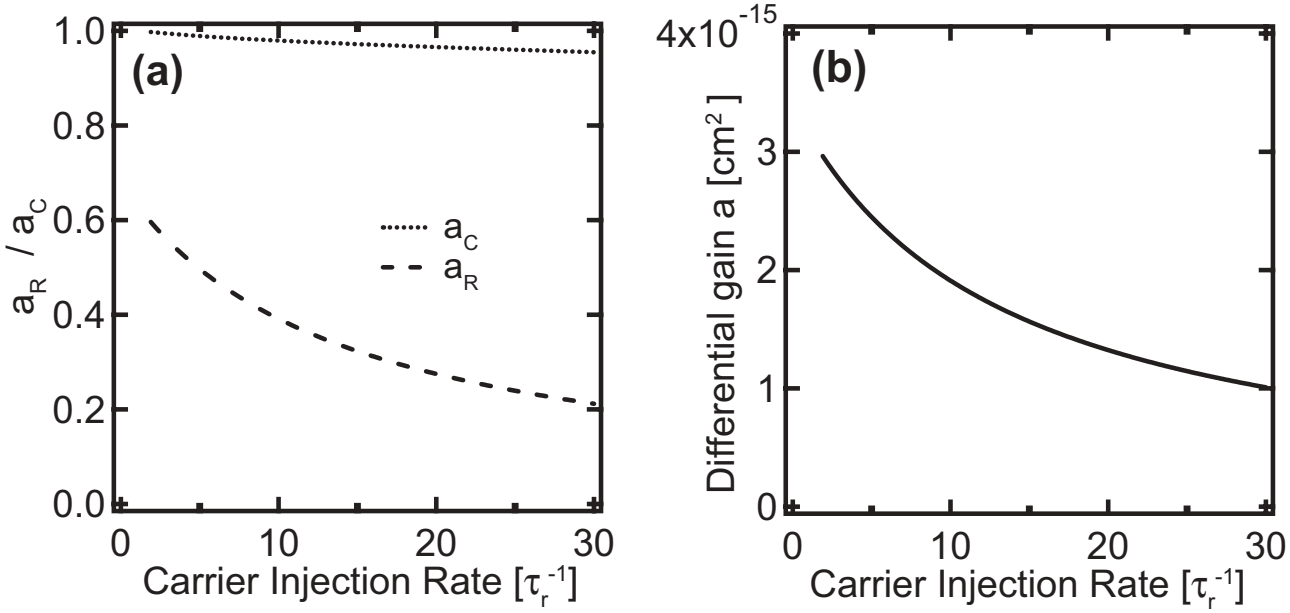

Fig. 6: Calculated a_r and a_c (a) and differential gain a (b) above threshold, as a function of injection rate in the 10-layer QD laser described in Ref. [14].

Next, we examine the effect of gain compression on the damping. Gain compression limits the damping of the laser response through the K factor if $\frac{\Gamma a_p}{a} \geq 1$ (see expression of K above). This term can be written analytically as a function of the bias point and is relevant for most practical situations. Figure 7(a) shows the calculated K factor for the same laser structure described above [14] for different intraband relaxation times.

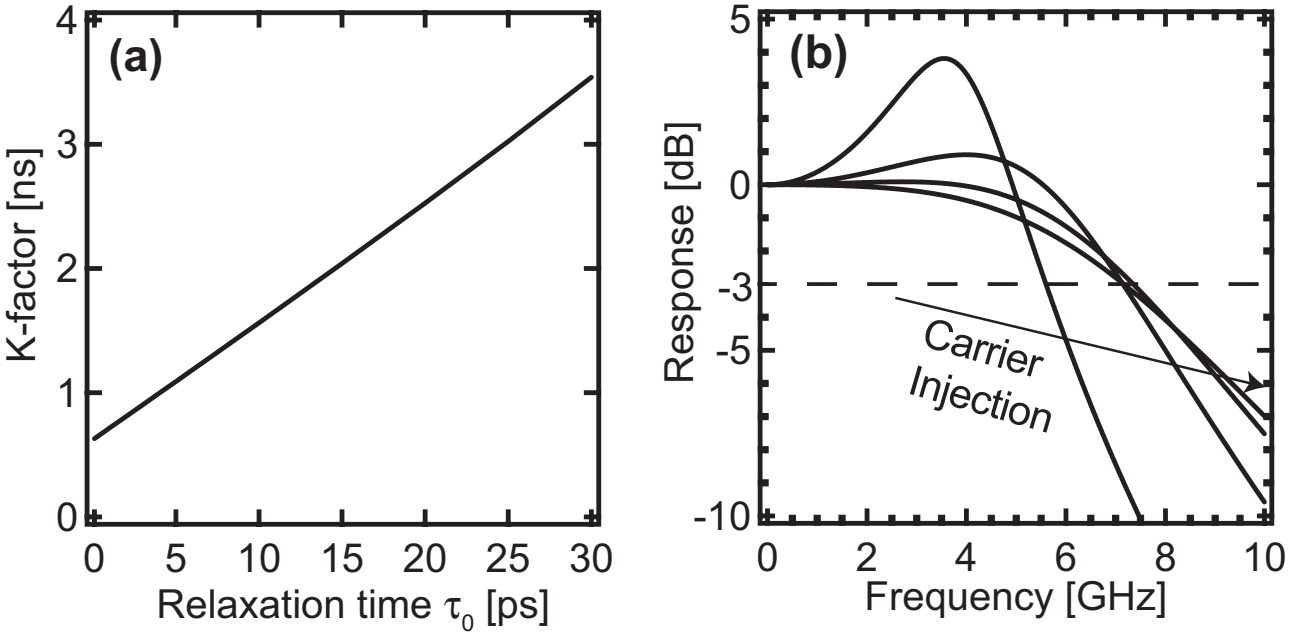

Fig. 7: (a) Calculated K factor as a function of relaxation time in the 10-layer QD laser described in Ref. [14]. (b) Calculated frequency response of the laser described in Ref. [14] for various injection rates.

The gain compression is also seen to be determined by intraband relaxation rather than capture. In fact, by comparing the terms in the analytical expression of K, it can be shown that the dominant term is the relaxation from ES to GS, which is not surprising in view of the preceding considerations.
With the values of differential gain and K-factor we can calculate the small-signal frequency response of the same laser for different bias points (Fig. 7(b)). The relaxation oscillation frequencies and K-factors calculated with this method agree well with the complete numerical calculation and with experimental results [1, 4, 3], assuming reasonable variations of the gain and relaxation time. We therefore conclude that this approach can lead to an accurate understanding of the modulation response of QD lasers, and particularly allows the identification of intraband relaxation as the main limiting factor of the laser bandwidth. We note that spectral hole burning is also expected to impact the dynamic characteristics through a reduction in the differential gain and an increase in the gain compression factor, as discussed in Section III. The quantitative evaluation of this effect will be the subject of future investigations.

Finally, we note that the carrier pile-up in nonlasing states has a significant impact not only on the amplitude, but also on the phase response of QD lasers. According to the ideal picture of QD gain as a Gaussian lineshape where the different energies correspond to GS transitions from dots of different sizes, the linewidth-enhancement factor α is expected to be zero at the gain peak, due to the antisymmetric relation between gain and refractive index (Kramers-Kronig relations). Values of $\alpha<1$ have indeed been measured by the Hakki-Paoli method at bias levels below threshold [15]. Nevertheless, the increase of ES population below and above threshold (Fig. 3(a)) produces a high-energy tail in the gain spectrum, which breaks the lineshape symmetry around the GS energy and can be expected to increase the α factor. This was indeed observed in measurements of the α factor above threshold in lasers with 3 QD layers (Fig. 9(a), Ref. [8]). The strong increase in α with bias above threshold is a peculiar characteristic of QD lasers, directly related to the relaxation bottleneck and to gain compression. In fact, the increasing ES population produces at the same time a decrease in the GS differential gain and an increase in the differential index, both factors contributing to an increase in

α. A simple calculation of the α factor has been made [8] by assuming both GS and ES to contribute a Gaussian lineshape, and calculating the differential refractive index as the Kramers-Kronig transform of the combined spectral gain. The result (Fig. 9(b)) is in good qualitative agreement with the experiment, confirming our understanding of the role of ES on the gain lineshape. For application in direct laser modulation, where low chirp and thus low α is needed, the increase of α can be avoided by the same design rules that maximize the differential gain: An increase of the number of QDs (thus of the saturated gain), to operate far from GS saturation, and a decrease of the intraband relaxation time. On the other hand, very large α-factor values can be obtained in QD lasers by working with a saturated GS gain (high loss): In this case the differential gain may approach zero and a pure phase modulation can be obtained [16], with possible application in phase modulators and all-optical switching [17]. The unique role of ES and intraband dynamics in QD lasers thus opens the way to gain shape engineering and to tuning device parameters in a much broader range than it is possible with quantum wells.

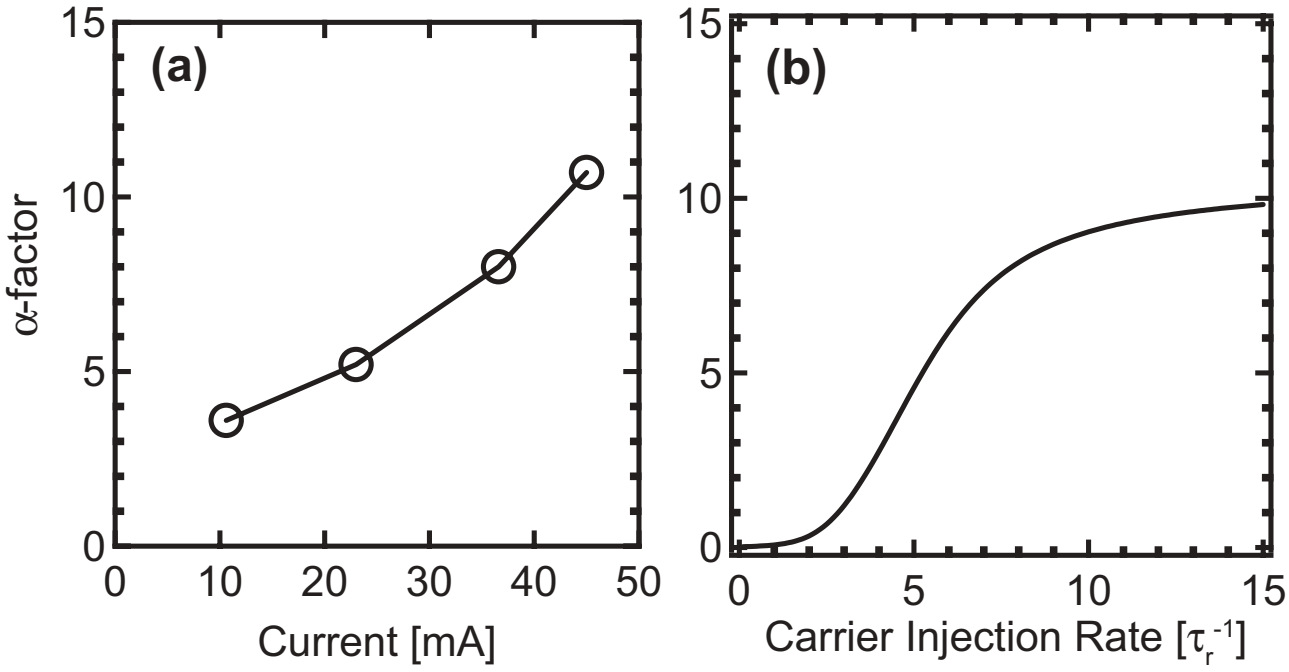

Fig. 8: (a) Measured α-factor in lasers with QD 3 layers (threshold current for this laser: 5 mA). (b) Corresponding calculation using Kramers-Kronig transform [8].

V. CONCLUSION

Three important aspects of intraband carrier dynamics in QD lasers emitting around 1300 nm have been analyzed: Intraband relaxation, capture and carrier localization. The relative impact of relaxation and capture has been assessed experimentally by the phenomenon of two-state lasing, which shows a strong carrier pile-up on the ES and thus a bottleneck in intradot relaxation, and allows an indirect but accurate determination of the relaxation time $\tau_0 \approx 5$-10 ps. The role of carrier localization on the establishment of quasi-thermal equilibrium has been investigated by measuring the stimulated and spontaneous emission spectra under lasing operation, allowing an order-of-magnitude estimation of the capture time, $\tau_c \approx 1$ ps, and of the homogeneous broadening $\Gamma_{hom} \approx 5$-10 meV. These parameters allow us to conclude that the electronic population is not in quasi-thermal equilibrium in a QD laser even at room temperature. The impact of capture and relaxation of the modulation response has been discussed by deriving an analytical expression for the differential gain and gain compression factor, which allow a thorough understanding of the modulation dynamics (relaxation oscillation frequency and damping). The effect of relaxation was also evidenced in the phase response, through unexpectedly high values of the linewidth enhancement factor. As a main conclusion, this extensive set of experimental and modeling results indicate that excited states and intradot relaxation play a major role in the characteristics of QD lasers and cannot be neglected even in first-order treatment. A more detailed analysis of the role of

spectral hole burning on the amplitude and phase response will be needed to provide a complete picture of QD laser dynamics.

ACKNOWLEDGEMENTS

This work was supported by the European Commission through the IST program, by the Swiss National Science Foundation, the SER-COST program, and the Swiss CTI-TOPNANO21 program. The authors are indebted to Dr. J.X. Chen for epitaxial growth, Dr. O. Gauthier-Lafaye and Dr. B. Thedrez (Alcatel CIT) for the measurements of the α-factor and interesting discussions, to Dr. Cyril Paranthoen for interesting discussions, and to Mr. V. Calligari for experimental help.

REFERENCES

1. R. Krebs, F. Klopf, S. Rennon, J.P. Reithmaier, and A. Forchel, Electron. Lett., **37,** 1223 (2001).
2. M. Kuntz, N.N. Ledentsov, D. Bimberg, A.R. Kovsh, V.M. Ustinov, A.E. Zhukov, and Y.M. Shernyakov, Appl Phys Lett, **81,** 3846 (2002).
3. M. Kuntz, G. Fiol, M. Lammlin, D. Bimberg, M.G. Thompson, K.T. Tan, C. Marinelli, A. Wonfor, R. Sellin, R.V. Penty, I.H. White, V.M. Ustinov, A.E. Zhukov, Y.M. Shernyakov, A.R. Kovsh, N.N. Ledentsov, C. Schubert, and V. Marembert, New J Phys, **6,** (2004).
4. M. Ishida, N. Hatori, T. Akiyama, K. Otsubo, Y. Nakata, H. Ebe, M. Sugawara, and Y. Arakawa, Appl Phys Lett, **85,** 4145 (2004).
5. A.V. Uskov, Y. Boucher, J. Le Bihan, and J. McInerney, Appl Phys Lett, **73,** 1499 (1998).
6. P. Bhattacharya and S. Ghosh, Appl Phys Lett, **80,** 3482 (2002).
7. A. Markus, J.X. Chen, C. Paranthoen, A. Fiore, C. Platz, and O. Gauthier-Lafaye, Appl Phys Lett, **82,** 1818 (2003).
8. A. Markus, J.X. Chen, O. Gauthier-Lafaye, J.-G. Provost, C. Paranthoen, and A. Fiore, IEEE J. Sel. Top. Quantum Electron., **9,** 1308 (2003).
9. A. Markus and A. Fiore, Phys. Stat. Sol. (a), **201,** 338 (2004).
10. M. Sugawara, K. Mukai, Y. Nakata, H. Ishikawa, and A. Sakamoto, Phys Rev B, **61,** 7595 (2000).
11. M. Grundmann, O. Stier, S. Bognar, C. Ribbat, F. Heinrichsdorff, and D. Bimberg, Phys Status Solidi A, **178,** 255 (2000).
12. A. Markus, M. Rossetti, V. Calligari, J.X. Chen, and A. Fiore, unpublished, (2005).
13. L.A. Coldren and S.W. Corzine, *Diode Lasers and Photonic Integrated Circuits*. Wiley Series in Microwave and Optical Engineering, ed. K. Chang. 1995, New York: John Wiley & Sons.
14. M. Kuntz, G. Fiol, M. Lammlin, C. Schubert, A.R. Kovsh, A. Jacob, A. Umbach, and D. Bimberg, Electronics Letters, **41,** 244 (2005).
15. T.C. Newell, D.J. Bossert, A. Stintz, B. Fuchs, K.J. Malloy, and L.F. Lester, Ieee Photonic Tech L, **11,** 1527 (1999).
16. B. Dagens, A. Markus, J.X. Chen, J.G. Provost, D. Make, O. Le Gouezigou, J. Landreau, A. Fiore, and B. Thedrez, Electronics Letters, **41,** 323 (2005).
17. A.V. Uskov, E.P. O'Reilly, R.J. Manning, R.P. Webb, D. Cotter, M. Laemmlin, N.N. Ledentsov, and D. Bimberg, Ieee Photonic Tech L, **16,** 1265 (2004).